Volume 1 | Number 1 | Jan 2013 | Pages 1–100

ChemComm

Chemical Communications
www.rsc.org/chemcomm

ROYAL SOCIETY OF CHEMISTRY

This is an *Accepted Manuscript*, which has been through the Royal Society of Chemistry peer review process and has been accepted for publication.

Accepted Manuscripts are published online shortly after acceptance, before technical editing, formatting and proof reading. Using this free service, authors can make their results available to the community, in citable form, before we publish the edited article. We will replace this *Accepted Manuscript* with the edited and formatted *Advance Article* as soon as it is available.

You can find more information about *Accepted Manuscripts* in the **Information for Authors**.

Please note that technical editing may introduce minor changes to the text and/or graphics, which may alter content. The journal's standard **Terms & Conditions** and the **Ethical guidelines** still apply. In no event shall the Royal Society of Chemistry be held responsible for any errors or omissions in this *Accepted Manuscript* or any consequences arising from the use of any information it contains.

Chemical Communications

COMMUNICATION

Synthesis and Characterization of Two-Dimensional Nb₄C₃ (MXene)

M. Ghidiu[a], M. Naguib[a], C. Shi[b], O. Mashtalir[a], L. M. Pan[c], B. Zhang[e], J. Yang[c,a,*], Y. Gogotsi[a], S. J. L. Billinge[b,d] and M. W. Barsoum[a,*]

We report on the synthesis of a phase-pure 2-dimensional ternary transition metal carbide (MXene), Nb₄C₃, only the second with formula M₄X₃, produced by etching of Nb₄AlC₃ in hydrofluoric acid. The structure was investigated with pair distribution function analysis. The resistivity of a cold-pressed disc was 0.0046 Ω•m, one of the most conductive MXenes to date.

Interest in two-dimensional (2D) materials has greatly increased in the past few years following the exploration of the properties of graphene and other materials such as hexagonal boron nitride and metal chalcogenides.[1,2] Recently, we have shown that the MAX phases - layered early transition metal ternary carbides and/or nitrides - can be transformed into their 2D counterparts (dubbed 'MXenes', denoting the removal of the A group element and emphasizing their analogy to graphene) through a fairly general process of chemical exfoliation with hydrofluoric acid (HF).[3,4] The general formula of the MAX phases is $M_{n+1}AX_n$, where M is an early transition metal, A is an A-group element, X is carbon and/or nitrogen, and n = 1, 2, or 3. With over 70 members – not including solid solutions - the MAX phase family is quite large. Given a general exfoliation route, this renders them ideal precursors for 2D materials with tuneable chemistries. The fact that the interlayer space can be readily intercalated by small and large cations as well as small organic molecules shows their potential for a large number of applications ranging from electrodes in batteries and supercapacitors[5,6,7] to sensors or reinforcements in polymers. When aqueous HF etching is carried out, the MXene surfaces are typically terminated by O, OH and/or F.[4,8] Because the stoichiometry of these terminations varies, the formula $M_{n+1}X_nT_x$, where T_x stands for a general surface termination, is used. Not surprisingly, atomistic

modelling predicts that these surface terminations are another powerful variable with which to control MXene properties.[9,10,11]

To date, we have reported on the following MXenes: $Ti_3C_2T_x$, Ti_2CT_x, $(Ti_{0.5},Nb_{0.5})_2CT_x$, $(V_{0.5},Cr_{0.5})_3C_2T_x$, Ti_3CNT_x, V_2CT_x, Nb_2CT_x, and $Ta_4C_3T_x$, with exploration of many others underway.[4,12,13] As this list shows, the main focus of synthesis has been on the M_2X (n = 1) and M_3X_2 (n = 2) phases. To date, $Ta_4C_3T_x$ is the only member reported where n = 3. $Nb_4C_3T_x$ was observed in the x-ray diffraction (XRD) patterns of Nb_2CT_x; however, it existed only as an impurity and was not isolated.[12] The purpose of this work was to prepare and isolate a phase-pure $Nb_4C_3T_x$ composition and report on its structure and resistivity, with special focus on pair distribution function analysis. This technique has proven useful for understanding the structure of MXenes on the nano scale, especially after intercalation.[8] This is pertinent to other MXenes, notably Nb_2CT_x, which have been observed to have, as a result of the etching process, larger than expected c parameters attributed to water intercalation.[12]

Polycrystalline Nb_4AlC_3 samples were prepared by *in-situ* hot pressing of commercial powders of Nb, Al and C at 1700 °C for 1 h under 30 MPa, as is described in the supporting information.[14] The resulting powders were predominantly single-phase Nb_4AlC_3 as determined by XRD (Fig. 1a). The Nb_4AlC_3 powder (< 38 μm particle size) was etched in 48-51 % aqueous HF for 96 h at ambient temperature, followed by washing with distilled water until pH ~ 5 was reached. The sediment was mixed in ethanol and allowed to dry by evaporation. A rudimentary yield by mass (mass of MXene products divided by starting mass of MAX) was 77 %. For this system it is important to note that this yield does not reflect molar quantities, since neither the nature of the MXene surface

terminations nor possible intercalant are precisely known. The number stated above simply indicates that the yields are robust.

Comparing the XRD pattern of the dried powder after etching (Fig. 1b) to its precursor, Nb_4AlC_3 (Fig. 1a), it is clear that the latter's peaks have disappeared and been replaced by a broadened (0002) peak at 2θ of 5.77°, corresponding to a *c* lattice parameter (*c*) of 3.059 nm. The original Nb_4AlC_3 (0002) peak occurs at 7.23° (2.242 nm). This more than 0.6 nm expansion along the [0001] was observed similarly for Nb_2CT_x and attributed to the intercalation of water layers or ions between the MXene sheets.[12]
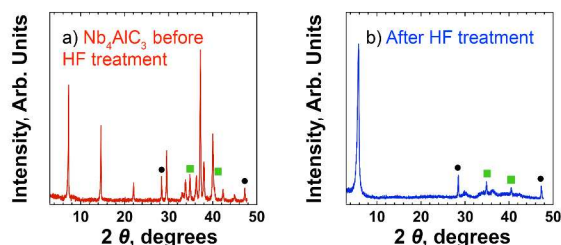

Figure 1. XRD diffraction patterns for Nb_4AlC_3 before (a) and after HF treatment (b). The black circles represent crystalline silicon added as an internal standard; the green squares represent NbC present as a phase impurity in the original Nb_4AlC_3 sample.

From energy-dispersive x-ray spectroscopy (EDS) analysis of the bulk Nb_4AlC_3 MAX and cold-pressed $Nb_4C_3T_x$ MXene discs, it is clear that there is a selective reduction in the Al content after etching; Al:Nb ratios decreased from roughly 0.16:1 to 0.03:1. Note that some of the remaining Al signal could originate from the reaction product, AlF_3, which may not have been fully washed away from the particles (this was observed in the case of Ti_3AlC_2), or from intercalated Al^{3+} ions.[3,5] C:Nb ratios increased from roughly 1.17:1 to 1.47:1 after etching. There is a rather large amount of C compared to the expected stoichiometry of 3 C: 4 Nb; however, this can arise from the similarity in energies of C K_α and Nb M_{IV} lines leading to peak overlap. Further, excess carbon could have been left after dissolution of some of the Nb and Al atoms, or even in the form of surface alkoxy groups due to ethanol washing as modelled by Enyashin and Ivanovskii.[15] As has been shown previously, a relatively large amount of F is likely bound to the MXene layers as surface termination.[4] There was also an increase in O signal; some of the oxygen present can be accounted for by oxygen-containing surface terminations (O or OH), and some is likely from water physisorbed between the layers. In addition, the fact that there is an overlap of O absorption edge with F emission may make some contribution.

Scanning-electron microscope (SEM) images of HF-treated grains (Fig. 2a) reveal the typical MXene morphology[3] that is similar to exfoliated graphite.[16] Transmission electron microscope (TEM) micrographs (Fig. 2b) also show typical MXene characteristics: flakes thin enough to be electron-transparent, as well as layering observed in cross-section. As seen in the right inset in Fig. 2b, the roughly 14 MXene layers in the section that are in total ~ 20 nm thick match well with the XRD results; the value of *c* for the (0002)

peak, 3.06 nm, gives roughly 1.5 nm per sheet. Selected-area electron diffraction (SAED – left inset) of a $Nb_4C_3T_x$ flake also confirms that – like all other MXenes – the hexagonal symmetry ($P6_3$/mmc) of the parent MAX phase persists after exfoliation.
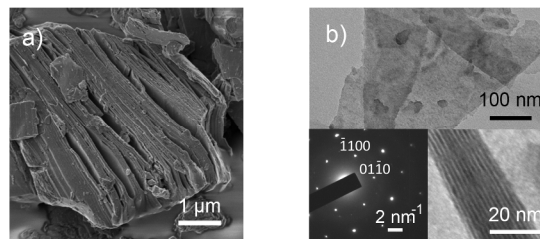

Figure 2. Electron microscopy of HF-treated Nb_4AlC_3: a) typical SEM micrograph showing an exfoliated grain; b) TEM micrograph of a $Nb_4C_3T_x$ flake. Left inset in (b) is a SAED pattern showing hexagonal basal plane symmetry. Right inset shows a cross-sectional TEM micrograph showing ~14 MXene layers with a total thickness of roughly 20 nm.

To gain further insight into the structure of $Nb_4C_3T_x$, atomic pair distribution function (PDF) analysis was carried out. This technique was recently used to characterize the structure of $Ti_3C_2T_x$ MXene.[8] Synchrotron X-ray total scattering experiments were conducted at beam line X17A at the National Synchrotron Light Source (NSLS) at Brookhaven National Laboratory with an X-ray energy of 67.42 keV (λ = 0.1839 Å).[17] The $Nb_4C_3T_x$ MXene and its MAX parent Nb_4AlC_3 were packed into kapton capillary tubes and measured at 100 K using a flowing nitrogen cryocooler. PDFgetX3[18] was used to correct and normalize the diffraction data and then apply a Fourier transform to obtain the experimental reduced pair distribution function, *G(r)*, according to

$$G(r) = 2/\pi \int_{Q_{min}}^{Q_{max}} Q[S(Q) - 1]\sin Qr dQ.$$

Here Q is the magnitude of the momentum transfer on scattering and $S(Q)$ is the properly corrected and normalized powder diffraction intensity measured from Q_{min} to Q_{max}.[19] $G(r)$ gives the probability of finding a pair of atoms separated by a distance of r. Structural modelling was carried out using the PDFgui[20] and SrFit[21] programs. The experimental pair distribution function of $Nb_4C_3T_x$ is shown in Fig. 3a. The sharp peaks observed over the entire range plotted indicate a well-ordered local structure.
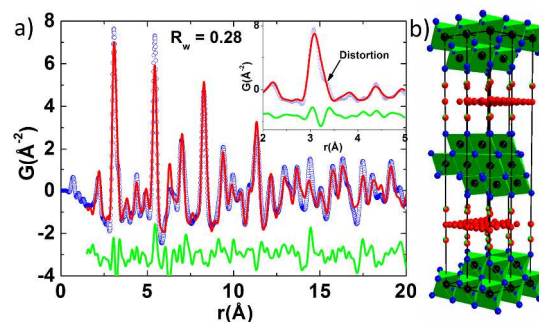

Figure 3. (a) Pair distribution function fit of $Nb_4C_3T_x$: blue circles are the measured data, the red solid line is the calculated pair distribution function of the best-fit structural model, and the green curve offset below is the

difference curve. The inset shows the expanded r-region from 2 Å to 5 Å where a shoulder peak at ~3.3 Å can be seen, indicating a distortion in the Nb_4C_3 slab. (b) The polyhedral representation of the undistorted $Nb_4C_3T_x$ structure. The Nb, C, O/F atoms are in blue, black, red/green colours. The intercalated water molecules are represented by sheets of oxygen atoms.

For the structural model, the space group $P6_3/mmc$ was used. The c (~3.1 nm) allows for two Nb_4C_3 slabs per unit cell. In the model the surface of the Nb_4C_3 slabs was terminated with O and F atoms as evidenced by the EDS results. Among three possible positions, i.e. $(0, 0, z)$, $(1/3, 2/3, z)$ and $(2/3, 1/3, z)$ for the terminating groups, as constrained by the space group, a better fit was obtained when the O/F atoms were placed on $(0, 0, z)$, yielding a ~1.5% lower agreement factor R_w than the other two alternatives. We further introduced a layer of water molecules between the slabs at Wyckoff positions 2b $(0, 0, 1/4)$, 2c $(1/3, 2/3, 1/4)$, 2d $(2/3, 1/3, 1/4)$, 6h $(x, 2x, 1/4)$ or 12j $(x, y, 1/4)$. The total amount of water is constrained by the oxygen content from EDS. The pair distribution function fit and structural model are displayed in Figure 3. Interestingly, a shoulder peak around ~3.3 Å (inset of Fig. 3a) was found for $Nb_4C_3T_x$ but wasn't captured by the model. Together with the overall poor fit of the undistorted model, this indicates the presence of a structural distortion within the Nb_4C_3 layer. Simple distorted models were tried without success, and more detailed models are being investigated at this time. This shoulder was not seen in the earlier pair distribution function study of $Ti_3C_2T_x$, whose layers are undistorted at the local scale.[8] More detail on the pair distribution function work, including the low-r region with the shoulder peak, is provided in the supporting information.

To compare this MXene to its parent phase and its previously-reported cousin Nb_2CT_x, powders of Nb_4AlC_3, Nb_2AlC, $Nb_4C_3T_x$ and Nb_2CT_x were cold-pressed under 1 GPa into discs (Nb_2AlC and Nb_2CT_x were synthesized according to previous work).[12] A four-point probe system was used to measure the bulk resistivity of the discs; these results are summarized in Table 1.

Table 1. Characteristics of Nb-containing MAX and MXene phases. Also listed are the values for $Ta_4C_3T_x$.

Sample	c (nm)	Thickness (mm)	Resistivity ($\Omega \cdot m$)
Nb_2AlC^*	1.388	0.678	$2.0 \cdot 10^{-5}$
Nb_4AlC_3	2.242	0.648	$3.3 \cdot 10^{-4}$
$Nb_2CT_x{}^*$	2.234	0.434	$6.1 \cdot 10^{-1}$
$Nb_4C_3T_x$	3.059	0.379	$4.6 \cdot 10^{-3}$
$Ta_4C_3T_x{}^\ddagger$	3.034	~ 0.3	$2.1 \cdot 10^{-2}$

* c values from ref. 12 $\ddagger$ All values from ref. 4

The measured resistivity was corrected for thickness and geometry (explained in the supporting information). As expected, the MAX phases Nb_4AlC_3 and Nb_2AlC showed lower resistivity than their exfoliated counterparts (MXenes involve the loss of metallic M-Al bonds from MAX Phases; Mauchamp *et al.* recently showed that within the basal plane of another MAX system, the plasmon behavior can be reproduced from an effective medium theory considering Cr_2AlC as an atomic scale superlattice built from pure Al and CrC planes[22]). For the MXenes, multilayer $Nb_4C_3T_x$ showed a lower resistivity than Nb_2CT_x, which can be rationalized by the

higher n value. MAX phases show high conductivity; $Nb_4C_3T_x$ ($n = 3$) has more MAX character due to the additional NbC layers compared to Nb_2CT_x ($n = 1$). The same trend was demonstrated between Ti_2CT_x and $Ti_3C_2T_x$.[4] Interestingly, and for reasons unclear at this time, the only other MXene with $n = 3$, $Ta_4C_3T_x$, shows a resistivity about 4.5 times higher than $Nb_4C_3T_x$. Note that MXenes have indeed shown higher conductivites in thin film form,[23] but we do not endeavour to make comparisons between those and our cold-pressed samples. As a final note, it is likely that oxidation of the MXenes could affect the resistivity. No long-term studies of the stability of either Nb_2CT_x or $Nb_4C_3T_x$ in air or water have yet been performed.

In summary, we have synthesized a phase-pure MXene, $Nb_4C_3T_x$, only the second with $n = 3$ reported to date. Its large c expansion of 0.617 nm is rationalized through water physisorption between the MXene layers, which is supported by a large increase in oxygen signal in EDS, as well as pair distribution function analysis, a technique that is proving invaluable to the study of these materials. $Nb_4C_3T_x$ further has a resistivity among the lowest reported for the MXene family in cold-pressed disc form.

Notes and references

^{a} Department of Materials Science and Engineering and A. J. Drexel Nanomaterials Institute, Drexel University, Philadelphia, Pennsylvania 19104.
^{b} Department of Applied Physics and Applied Mathematics, Columbia University, New York, New York 10027, USA.
^{c} College of Materials Science and Engineering, Nanjing Tech University, Nanjing 210009, China
^{d} Condensed Matter Physics and Materials Science Department, Brookhaven National Laboratory, Upton, New York 11973, USA.

Acknowledgements

1. K. S. Novoselov, D. Jiang, F. Schedin, T. J. Booth, V. V. Khotkevich, S. V. Morozov, and A. K. Geim, *Proc. Natl. Acad. Sci. U. S. A.*, 2005, **102**, 10451–10453.
2. J. N. Coleman, M. Lotya, A. O'Neill, S. D. Bergin, P. J. King, U. Khan, K. Young, A. Gaucher, S. De, R. J. Smith, I. V. Shvets, S. K. Arora, G. Stanton, H.-Y. Kim, K. Lee, G. T. Kim, G. S. Duesberg, T. Hallam, J. J.

Boland, J. J. Wang, J. F. Donegan, J. C. Grunlan, G. Moriarty, A. Shmeliov, R. J. Nicholls, J. M. Perkins, E. M. Grieveson, K. Theuwissen, D. W. McComb, P. D. Nellist, and V. Nicolosi, *Science*, 2011, **331**, 568–571.

3. M. Naguib, M. Kurtoglu, V. Presser, J. Lu, J. Niu, M. Heon, L. Hultman, Y. Gogotsi, and M. W. Barsoum, *Adv. Mater.*, 2011, **23**, 4248–4253.

4. M. Naguib, O. Mashtalir, J. Carle, V. Presser, J. Lu, L. Hultman, Y. Gogotsi, and M. W. Barsoum, *ACS Nano*, 2012, **6**, 1322–1331.

5. M. R. Lukatskaya, O. Mashtalir, C. E. Ren, Y. Dall'Agnese, P. Rozier, P. L. Taberna, M. Naguib, P. Simon, M. W. Barsoum, and Y. Gogotsi, *Science*, 2013, **341**, 1502–1505.

6. M. Naguib, J. Come, B. Dyatkin, V. Presser, P.-L. Taberna, P. Simon, M. W. Barsoum, and Y. Gogotsi, *Electrochem. Commun.*, 2012, **16**, 61–64.

7. O. Mashtalir, M. Naguib, V. N. Mochalin, Y. Dall'Agnese, M. Heon, M. W. Barsoum, and Y. Gogotsi, *Nat. Commun.*, 2013, **4**, 1716.

8. C. Shi, M. Beidaghi, M. Naguib, O. Mashtalir, Y. Gogotsi, and S. J. L. Billinge, *Phys. Rev. Lett.*, 2014, **112**, 125501.

9. Q. Tang, Z. Zhou, and P. Shen, *J. Am. Chem. Soc.*, 2012, **134**, 16909–16916.

10. M. Khazaei, M. Arai, T. Sasaki, M. Estili, and Y. Sakka, *Phys. Chem. Chem. Phys.*, 2014, **16**, 7841–7849.

11. Y. Xie and P. R. C. Kent, *Phys. Rev. B*, 2013, **87**, 235441.

12. M. Naguib, J. Halim, J. Lu, K. M. Cook, L. Hultman, Y. Gogotsi, and M. W. Barsoum, *J. Am. Chem. Soc.*, 2013, **135**, 15966–15969.

13. M. Naguib, V. N. Mochalin, M. W. Barsoum, and Y. Gogotsi, *Adv. Mater.*, 2014, **26**, 992–1005.

14. C. Hu, F. Li, L. He, M. Liu, J. Zhang, J. Wang, Y. Bao, J. Wang, and Y. Zhou, *J. Am. Ceram. Soc.*, 2008, **91**, 2258–2263.

15. A. N. Enyashin and A. L. Ivanovskii, *J. Phys. Chem. C*, 2013, **117**, 13637–13643.

16. D. Chung, *J. Mater. Sci.*, 1987, **22**, 4190–4198.

17. P. J. Chupas, X. Qiu, J. C. Hanson, P. L. Lee, C. P. Grey, and S. J. L. Billinge, *J. Appl. Crystallogr.*, 2003, **36**, 1342–1347.

18. P. Juhás, T. Davis, C. L. Farrow, and S. J. L. Billinge, *J. Appl. Crystallogr.*, 2013, **46**, 560–566.

19. T. Egami and S. J. L. Billinge, *Underneath the Bragg peaks: structural analysis of complex materials*, Elsevier, Amsterdam, 2nd edn., 2012.

20. C. L. Farrow, P. Juhas, J. W. Liu, D. Bryndin, E. S. Božin, J. Bloch, Th. Proffen, and S. J. L. Billinge, *J. Phys. Condens. Matter*, 2007, **19**, 335219.

21. C. L. Farrow, P. Juhás, and S. J. L. Billinge, *SrFit*, 2010.

22. V. Mauchamp, M. Bugnet, P. Chartier, T. Cabioc'h, M. Jaouen, J. Vinson, K. Jorissen, and J. J. Rehr, *Phys. Rev. B*, 2012, **86**, 125109.

23. J. Halim, M. R. Lukatskaya, K. M. Cook, J. Lu, C. R. Smith, L.-Å. Näslund, S. J. May, L. Hultman, Y. Gogotsi, P. Eklund, and M. W. Barsoum, *Chem. Mater.*, 2014, **26**, 2374–2381.